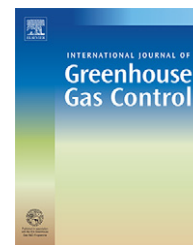


available at [www.sciencedirect.com](http://www.sciencedirect.com)journal homepage: [www.elsevier.com/locate/ijggc](http://www.elsevier.com/locate/ijggc)

# A method for quick assessment of CO<sub>2</sub> storage capacity in closed and semi-closed saline formations

Quanlin Zhou<sup>\*</sup>, Jens T. Birkholzer, Chin-Fu Tsang, Jonny Rutqvist

Earth Sciences Division, Lawrence Berkeley National Laboratory, University of California, One Cyclotron Road, MS 90-1116, Berkeley, CA 94720, USA

## ARTICLE INFO

### Article history:

Received 5 November 2007

Received in revised form

5 February 2008

Accepted 7 February 2008

Published on line 21 March 2008

### Keywords:

Geological CO<sub>2</sub> sequestration

Storage capacity

Saline aquifer

Pressure buildup

Numerical simulation

## ABSTRACT

Saline aquifers of high permeability bounded by overlying/underlying seals may be surrounded laterally by low-permeability zones, possibly caused by natural heterogeneity and/or faulting. Carbon dioxide (CO<sub>2</sub>) injection into and storage in such “closed” systems with impervious seals, or “semi-closed” systems with non-ideal (low permeability) seals, is different from that in “open” systems, from which the displaced brine can easily escape laterally. In closed or semi-closed systems, the pressure buildup caused by continuous industrial-scale CO<sub>2</sub> injection may have a limiting effect on CO<sub>2</sub> storage capacity, because geomechanical damage caused by overpressure needs to be avoided. In this research, a simple analytical method was developed for the quick assessment of the CO<sub>2</sub> storage capacity in such closed and semi-closed systems. This quick-assessment method is based on the fact that native brine (of an equivalent volume) displaced by the cumulative injected CO<sub>2</sub> occupies additional pore volume within the storage formation and the seals, provided by pore and brine compressibility in response to pressure buildup. With non-ideal seals, brine may also leak through the seals into overlying/underlying formations. The quick-assessment method calculates these brine displacement contributions in response to an estimated average pressure buildup in the storage reservoir. The CO<sub>2</sub> storage capacity and the transient domain-averaged pressure buildup estimated through the quick-assessment method were compared with the “true” values obtained using detailed numerical simulations of CO<sub>2</sub> and brine transport in a two-dimensional radial system. The good agreement indicates that the proposed method can produce reasonable approximations for storage-formation-seal systems of various geometric and hydrogeological properties.

© 2008 Elsevier Ltd. All rights reserved.

## 1. Introduction

Geological carbon dioxide (CO<sub>2</sub>) sequestration in deep formations (e.g., saline aquifers, gas and oil reservoirs, and coal beds) is a promising measure for mitigating the impact of climate change (Bachu et al., 1994; Bachu, 2002; Koide et al., 1992; IPCC, 2005; Van der Meer, 1992). Reliable estimates are needed for the CO<sub>2</sub> storage capacity of geologic basins (Bradshaw et al., 2007). Currently, basin-scale storage capacity is often esti-

mated based on the effective pore volume of suitable formations (i.e., those formations with sufficient injectivity, size, and long-term CO<sub>2</sub> containment capability). The effectiveness, or the storage efficiency factor, of suitable formations describes the fraction of total pore space available for CO<sub>2</sub> storage, limited by heterogeneity, buoyancy effects, residual water saturation, etc. (Bachu and Adams, 2003). Guidelines for estimating the storage capacity of deep saline formations were recently developed by the Capacity and

<sup>\*</sup> Corresponding author. Tel.: +1 510 486 5748; fax: +1 510 486 5686.

E-mail address: [qzhou@lbl.gov](mailto:qzhou@lbl.gov) (Q. Zhou).

1750-5836/\$ – see front matter © 2008 Elsevier Ltd. All rights reserved.

doi:10.1016/j.ijggc.2008.02.004

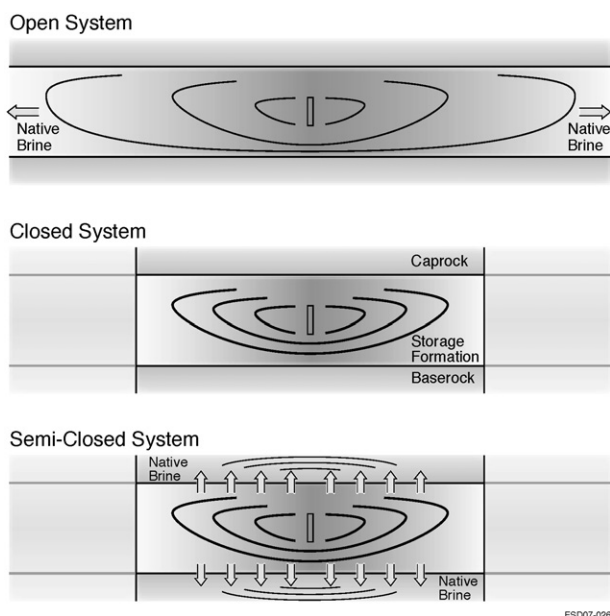


**Fig. 1 – Schematic showing open systems vs. closed or semi-closed systems (not to scale).**

Fairways Subgroup of the Geological Working Group of the U.S. Department of Energy (USDOE) Carbon Sequestration Regional Partnerships (USDOE, 2007). The current practice generally involves estimating storage capacity of “open” formations (Fig. 1, top), from which the native fluid can easily escape laterally and make room for the injected  $\text{CO}_2$  (e.g., Doughty and Pruess, 2004; Holloway et al., 1996; Shafeen et al., 2004; Van der Meer, 1995). For such open formations, the pressure buildup caused by  $\text{CO}_2$  injection is usually not a limiting factor except for maximum bottom-hole pressure at the injection well. However, the large amount of native brine laterally displaced by injected  $\text{CO}_2$  in open systems may have a hydrological and geochemical impact on shallow groundwater resources (Birkholzer et al., 2007; Nicot, 2008), an issue not addressed directly in this paper.

In certain geological situations, a storage basin may be composed of a number of compartmentalized reservoirs laterally separated by low-permeability zones. These zones may be formed by natural heterogeneity and/or faulting. When such a reservoir, bounded vertically by impervious seals, is surrounded on all sides by barriers of very low permeability, this reservoir acts as a “closed” system (Fig. 1, middle) (i.e., there is negligible hydraulic communication with other formations during the injection period of interest, usually 30–50 years). Evidence of such closed systems has been found in hydrocarbon reservoirs, as indicated by sharp changes in fluid pressure along their boundaries (Muggeridge et al., 2004; Neuzil, 1995; Puckette and Al-Shaieb, 2003). Examples of such closed systems also include natural  $\text{CO}_2$  reservoirs of high purity, which can be used as analogues for geological  $\text{CO}_2$  sequestration (e.g., Allis et al., 2001; Pearce et al., 1996; Stevens et al., 2001). When large volumes of  $\text{CO}_2$  are injected into a compartmentalized formation, which acts like a closed system (with the time scale of interest being the  $\text{CO}_2$  injection period), a significant pressure buildup will be

produced (e.g., Holloway et al., 1996; Polak et al., 2004). This pressure buildup can severely limit the  $\text{CO}_2$  storage capacity, because overpressure-associated geomechanical damage needs to be avoided (Rutqvist and Tsang, 2002; Rutqvist et al., 2007). In this case, the storage capacity mainly depends on pore and brine compressibilities that provide expanded pore space available for storing the injected  $\text{CO}_2$ , and on the maximum pressure buildup that the formation can sustain.

Of course, the overlying and underlying seals of a storage aquifer are not perfectly impervious, allowing the pressure buildup caused by  $\text{CO}_2$  injection and storage to partially dissipate into and through these seals. In this case, the saline aquifer acts like a “semi-closed” system (Fig. 1, bottom), allowing some fraction of the displaced brine to migrate into and through the overlying and underlying sealing units, which in turn would increase the storage capacity for  $\text{CO}_2$ . (Meanwhile, the stored  $\text{CO}_2$  is safely contained within the storage formation because of permeability and capillary barriers.) The importance of this vertical interlayer communication mostly depends on the permeability of the seals, which can vary widely (from  $10^{-23}$  to  $10^{-16} \text{ m}^2$ , or from  $10^{-8}$  to  $10^{-1} \text{ mD}$ ) depending on their hydrogeological characteristics (e.g., Domenico and Schwartz, 1998; Hart et al., 2006; Hovorka et al., 2001; Neuzil, 1994). Relatively permeable sealing units (e.g., with permeability on the order of  $10^{-18} \text{ m}^2$  or higher) may allow considerable vertical brine leakage out of the storage reservoir over the injection period. In this case, the pressure buildup may be reduced, and pressure constraints may not be a limiting factor in  $\text{CO}_2$  storage.

Our research aims at developing a method for the quick assessment of  $\text{CO}_2$  storage capacity in deep closed and semi-closed saline formations, complementing existing methods for capacity estimates in open systems (USDOE, 2007). This method can be used to estimate the storage efficiency factor and the transient domain-averaged pressure buildup. The validity of the method is demonstrated by comparing the estimated storage capacities to the “true” values calculated through detailed modeling of multiphase flow and multi-component transport of  $\text{CO}_2$  and brine. The modeling was conducted using the TOUGH2/ECO2N code, which has been tested and compared with other codes (Pruess, 2005; Pruess et al., 2004). The validity range is demonstrated for a range of hypothetical formation–seal systems, with varying lateral radial extent (i.e., pore volume) and hydrogeological properties (i.e., permeability and pore compressibility) of the storage formation and sealing units.

## 2. A quick-assessment method for $\text{CO}_2$ storage capacity

We developed a simple method for assessing the storage capacity of closed and semi-closed storage formations. The basic principle is that  $\text{CO}_2$  injection into these systems will lead to pressurization (pressure buildup), because an additional volume of fluid needs to be stored. The injected  $\text{CO}_2$  displaces an equivalent volume of native brine, which may either (1) be stored in the expanded pore space in the storage formation, (2) be stored in the expanded pore space in the seals, or (3) leak through the seals into overlying/underlying

formations. The quick-assessment method predicts the pressure-buildup history over a given injection period and the “actual” storage efficiency factor at the end of injection. We define the storage efficiency factor,  $E$ , as the volumetric fraction of stored  $\text{CO}_2$ , per unit initial total pore volume of the storage formation, similar to the earlier definition for open systems (USDOE, 2007). The method is designed to provide capacity estimates at early stages of site selection and characterization, when (1) quick assessments of multiple sites may be needed and (2) site characterization data are rather sparse. More specifically, the estimated pressure increase caused by injection and storage of a specified volume of  $\text{CO}_2$  can be compared to a sustainable pressure threshold, which is the maximum pressure that the formation can sustain without geomechanical damage. Alternatively, one may determine the maximum  $\text{CO}_2$  volume that can be injected without jeopardizing the geomechanical structure of the formation–seal system.

### 2.1. Simplifications and assumptions

Several simplifications and assumptions of both reservoir characteristics (geometric and hydrogeological properties) and processes made in the quick-assessment method are outlined below for an idealized, two-dimensional radial formation–seal system:

- The homogeneous storage formation for  $\text{CO}_2$  sequestration is of radial extent  $R$  and thickness  $B_f$ , with an initial porosity  $\phi_f$ . The initial total pore volume is  $V_f = \phi_f AB_f = \pi R^2 \phi_f B_f$ , where  $A$  is the horizontal area. The storage formation has a pore compressibility  $\beta_p (= 1/\phi_f (\partial \phi_f / \partial p))$ , where  $\phi_f$  is the storage formation porosity, dependent on pressure change), which includes the possible contribution of vertical formation expansion and reflects the confining pressure and overburden stress prior to  $\text{CO}_2$  injection.
- The upper and lower homogeneous seals have a uniform, identical thickness,  $B_s$ , permeability  $k_s$ , porosity  $\phi_s$ , and pore compressibility  $\beta_{ps}$ . The total pore volume of both seals is  $V_s = 2\phi_s AB_s$ .
- The native brine has compressibility,  $\beta_w (= 1/\rho_w (\partial \rho_w / \partial p))$ , representing the change in brine density,  $\rho_w$ , in response to pressure buildup, and viscosity,  $\mu_w$ , dependent on temperature, pressure, and salinity at the initial time of injection.
- The above hydrogeological parameters are assumed to be constant over the relevant range of pressure conditions, from the initial hydrostatic pressure to the elevated pressure value under final storage conditions. Only porosity changes are considered in response to pressure increases.
- The storage formation has uniform pressure buildup at any time of injection, independent of formation permeability. This overpressure decreases linearly through the seals to the hydrostatic pressure (prior to  $\text{CO}_2$  injection) assumed at the top of the overlying seal and at the bottom of the underlying seal.
- All injected  $\text{CO}_2$  mass is contained as a  $\text{CO}_2$ -rich phase, with negligible dissolved  $\text{CO}_2$  mass within the storage formation. The total volume of stored  $\text{CO}_2$  depends on  $\text{CO}_2$  density, which in turn depends on temperature and transient pressure conditions.

- Native brine leakage occurs through the entire formation–seal interface with a uniform leakage rate, independent of  $\text{CO}_2$  plume extent.

The validity of some of these assumptions is discussed in Section 4, based on the detailed simulation results presented in Section 3. Note that the storage formation can have any shape with varying thickness, because only its total pore volume is used in the quick-assessment method. Specifications on the geometry of the storage formation have been chosen for easier comparison with numerical simulation results.

### 2.2. Basic equations

The quick-assessment method considers that the pore volume needed to store injected  $\text{CO}_2$ ,  $V_{\text{CO}_2}(t_i)$ , after a given injection time,  $t_i$ , is provided by three contributions: (1) the expanded storage volume in the storage formation resulting from pressure buildup, (2) the expanded storage volume within the seals resulting from pressure buildup, and (3) the volumetric leakage of brine into the formations above the upper seal and below the lower seal. The expanded storage volume is caused by both brine and pore compressibility. A simple expression describes this volumetric relationship, as follows:

$$V_{\text{CO}_2}(t_i) = (\beta_p + \beta_w)\Delta p(t_i)V_f + 0.5(\beta_{ps} + \beta_w)\Delta p(t_i)V_s + \int_0^{t_i} \frac{2Ak_s \Delta p(t)}{\mu_w B_s} dt, \quad (1)$$

where  $\Delta p(t_i)$  is the pressure buildup at time  $t_i$ ,  $\Delta p(t)$  ( $t = [0, t_i]$ ) is the transient pressure buildup from the beginning to the end of injection, and the factor of 0.5 stems from the assumption of linear pressure buildup from zero at the top of the overlying seal (and the bottom of the underlying seal) to the storage-formation value at the formation–seal interfaces. Each of the three terms on the right-hand side of Eq. (1) corresponds to one of the three storage contributions mentioned above. Eq. (1) essentially links  $V_{\text{CO}_2}(t_i)$  to the average pressure buildup in the storage formation. By solving Eq. (1) for  $t_i$ , the total pressure buildup in the closed or semi-closed formation can be assessed as a function of  $V_{\text{CO}_2}(t_i)$ .

Based on the definition of the storage efficiency factor and Eq. (1), the storage efficiency factor,  $E(t_i)$ , for a semi-closed system can be calculated:

$$E(t_i) = (\beta_p + \beta_w)\Delta p(t_i) + 0.5(\beta_{ps} + \beta_w)\frac{V_s}{V_f}\Delta p(t_i) + \int_0^{t_i} \frac{2Ak_s \Delta p(t)}{\mu_w B_s V_f} dt, \quad (2)$$

where the storage efficiency factor consists of three individual efficiency contributions from expanded pore volume in the storage formation and the seals, as well as from brine leakage into the underlying and overlying formations. To compare the relative importance of the three individual contributions, we define the volumetric fractions of displaced brine stored in the

storage formation ( $F_f$ ), in the seals ( $F_s$ ), and in the overlying/underlying formations ( $F_l$ ), relative to the total pore volume storing  $\text{CO}_2$ , as follows:

$$F_f = \frac{(\beta_p + \beta_w)\Delta p(t_f)V_f}{V_{\text{CO}_2}(t_f)}, \quad (3a)$$

$$F_s = \frac{0.5(\beta_{ps} + \beta_w)\Delta p(t_f)V_s}{V_{\text{CO}_2}(t_f)}, \quad (3b)$$

$$F_l = \int_0^{t_f} \frac{2Ak_s\Delta p(t)/\mu_w B_s dt}{V_{\text{CO}_2}(t_f)}. \quad (3c)$$

By definition,  $F_f$ ,  $F_s$ , and  $F_l$  add up to one. Note that from these volumetric fractions, one can calculate the total volumes of the displaced brine leaking into other formations and stored in the seals and the storage formation, by multiplying these fractions by the volume of stored  $\text{CO}_2$  at the final storage condition.

Note that  $V_{\text{CO}_2}$  is not the total volume of  $\text{CO}_2$  at the injection condition; it is the total pore volume occupied by injected  $\text{CO}_2$  under the final storage condition, depending on the density of  $\text{CO}_2$ -rich phase. The necessary  $\text{CO}_2$  storage capacity for a given site is often provided in total  $\text{CO}_2$  mass,  $M_{\text{CO}_2}$ , instead of  $V_{\text{CO}_2}$ . Conversion of volume to mass is achieved through  $M_{\text{CO}_2} = \rho_{\text{CO}_2}(t_f)V_{\text{CO}_2}$ , in which the  $\text{CO}_2$  density,  $\rho_{\text{CO}_2}$ , is evaluated at pressures and temperatures representing the final storage conditions. Because the pressure buildup caused by injection is not known beforehand for a given total  $\text{CO}_2$  mass, the  $\text{CO}_2$  density at storage conditions is either estimated a priori (in anticipation of an estimated pressure buildup) or determined in an iterative procedure, using the calculated average pressure to correct the density and vice versa.

### 2.3. Application to closed systems

In a closed system, the available volume for storage of  $\text{CO}_2$  is provided only by the expansion of the pore volume and the increased brine density in response to pressure buildup in the storage formation. Eq. (1) can then be simplified to the following linear expression:

$$V_{\text{CO}_2}(t_f) = (\beta_p + \beta_w)\Delta p(t_f)V_f. \quad (4)$$

This equation can be used, for example, to estimate the maximum storage capacity for a given sustainable pressure buildup,  $\Delta p_{\text{max}}$ . Similarly, one can calculate the expected average pressure buildup,  $\Delta p(t_f)$ , for a given total volume of stored  $\text{CO}_2$  or a given  $\text{CO}_2$  mass.

The storage efficiency factor of  $\text{CO}_2$  storage in a closed system with average pressure buildup  $\Delta p(t_f)$  can be derived from a simplification of Eq. (2)

$$E = E_p(\Delta p(t_f)) + E_b(\Delta p(t_f)) = (\beta_p + \beta_w)\Delta p(t_f), \quad (5)$$

where  $E_p$  is the storage efficiency factor caused by pore compressibility, and  $E_b$  is the storage efficiency factor produced from brine compressibility. Inserting the sustainable pressure buildup,  $\Delta p_{\text{max}}$ , into Eq. (5) results in the maximum storage efficiency. For example, using  $\Delta p_{\text{max}} = 6.0$  MPa, a pore compressibility of  $4.5 \times 10^{-10} \text{ Pa}^{-1}$  and a brine compressibility of  $3.5 \times 10^{-10} \text{ Pa}^{-1}$ , we arrive at  $E_p = 0.0027$  and  $E_b = 0.0021$ , and  $E = 0.0048$ . In other words, less than half a percent of the total pore volume of a closed system would be available for the volumetric storage of  $\text{CO}_2$  in a closed system during the injection period.

### 2.4. Application to semi-closed systems

Unlike the linear relationship of the total volumetric storage capacity and pressure buildup to pore and brine compressibilities for a closed system, such relationships for a semi-closed system are nonlinear and transient, with the pressure buildup in the storage formation affecting leakage rate through the seals, and vice versa. This makes solving of Eq. (1) more complicated; however, a solution can be achieved through a simple numerical integration in time. For this purpose, the injection time period  $[0, t_f]$  can be discretized into a number ( $n$ ) of equally spaced time intervals of duration  $\Delta t$  to form a time series:  $t_0, t_1, \dots, t_{i-1}, t_i, \dots, t_{n-1}, t_n$ , with  $t_0 = 0$  and  $t_n = t_f$ . Eq. (1) converts into its discrete form as follows:

$$\Delta p(t_i) = \frac{V_{\text{CO}_2}(t_i) - 2Ak_s\Delta t/\mu_w B_s \sum_{j=0}^{i-1} \Delta p(t_j)}{(\beta_p + \beta_w)V_f + 0.5(\beta_{ps} + \beta_w)V_s + Ak_s\Delta t/\mu_w B_s}, \quad i = [1, n] \quad (6)$$

At each new time step, the pressure-buildup values at all previous time steps are known, such that the summation term in Eq. (6) (representing the cumulative brine leakage from beginning of injection to the previous time step) can be executed. Eq. (6) eventually yields the pressure buildup at all time steps from the beginning to the end of injection. Once Eq. (6) has been solved, the storage efficiency factors in Eq. (2) or the volumetric fractions in Eq. (3) can be derived using the known injection and pressure history.

In the quick-assessment method, it is assumed that the semi-closed systems have a radial impervious layer to bound the systems laterally. This method may not be applicable to the systems bounded laterally by a permeable layer with a permeability value between those of the storage formation and the overlying/underlying sealing units.

Note that continued  $\text{CO}_2$  injection into a semi-closed system would eventually lead to a steady-state condition at which the volumetric injection rate,  $Q_{\text{CO}_2}$  (as a function of the steady-state storage condition), equals the rate of displaced brine leakage through the seals, assuming that the geomechanical and hydraulic integrity of the storage unit and seals is maintained. The pressure buildup,  $\Delta p_s$ , associated with this steady-state condition can be calculated as follows:

$$\Delta p_s = \frac{Q_{\text{CO}_2}}{2Ak_s/\mu_w B_s}, \quad Q_{\text{CO}_2} = \frac{G_{\text{CO}_2}}{\rho_{\text{CO}_2}(\Delta p_s)}, \quad (7)$$



where  $G_{CO_2}$  is the injection rate of  $CO_2$  mass. If  $\Delta p_s$  is unrealistically high, i.e., higher than the sustainable pressure buildup, the storage capacity is pressure-constrained and needs to be evaluated, using Eq. (6). If, on the other hand,  $\Delta p_s$  is relatively small, brine leakage through the seals is sufficient to allow for significant  $CO_2$  storage without pressurization concerns. In this case, the semi-closed system acts like an open storage formation, and its storage capacity is not pressure-constrained.

### 2.5. Sustainable pressure buildup

The  $CO_2$  storage capacity of pressure-constrained systems depends on the sustainable pressure buildup that a given formation–seal system is expected to tolerate without geomechanical degradation (such as microfracturing and/or fault reactivation) of the sealing structures (USEPA, 1994; Neuzil, 2003; Rutqvist and Tsang, 2002; Rutqvist et al., 2007). Fluid pressure in the storage formation may also be constrained to limit the pressure driving forces into neighboring formations, or to account for potential concerns about seismicity. According to Rutqvist et al. (2007), the sustainable pressure buildup should be reviewed on a case-by-case basis, taking into account initial stress fields and geomechanical properties of the rock units at the selected sites.

Some guidance on the determination of a sustainable pressure buildup (for geomechanical damage) is provided by the current practice for underground injection control of liquid wastes. The regulatory standard states that maximum injection pressure should be less than the measured fracture-closure pressure. Below the fracture-closure pressure, any existing fractures cannot open and no new fractures can form, implying no enhanced migration of waste fluids out of the injection intervals (USEPA, 1994). The regional guidance for implementation is that the maximum injection pressures can be determined either by a site-specific fracture-closure pressure derived from direct or indirect testing, or by formation-specific default values for the fracture-closure pressure gradients. For example, a default value of  $0.0129 \text{ MPa m}^{-1}$  (130% of the hydrostatic pressure gradient) is given for the Mt. Simon Formation in Illinois, USA;  $0.0181 \text{ MPa m}^{-1}$  (181% of the hydrostatic pressure gradient) is reported for the Dundee Limestone in the Michigan Basin in USA. These fracture-closure pressure gradients correspond to sustainable fluid pressures of 15.5 and 21.7 MPa at 1200 m depth, leading to sustainable pressure buildup of 3.5 and 9.7 MPa, respectively. In the following example applications, we chose a sustainable pressure buildup of 6.0 MPa, which corresponds to 50% of the initial hydrostatic pressure at the top (1200 m) of the hypothetical storage formation. This value was used to demonstrate the quick-assessment method, and a site-specific value is needed when applied to a specific geologic site.

## 3. Numerical simulations and results

To validate the quick-assessment method discussed above, the “true”  $CO_2$  storage capacity of closed or semi-closed formations was calculated through numerical simulation of

the multiphase flow and multicomponent transport of  $CO_2$  and brine in a hypothetical deep saline formation, using the TOUGH2/ECO2N simulator (Pruess, 2005; Pruess et al., 1999). The validity range of the quick-assessment method was demonstrated using different simulation runs, varying the radial extent to evaluate the effect of storage formation size, varying storage-formation properties to evaluate the uniformity of pressure buildup, and varying seal permeability to investigate the effect of brine leakage into and through the seals and its impact on storage capacity. For each simulation run, we calculated the storage efficiency factor ( $E$ ) and the domain-averaged pressure buildup. If the simulated pressure buildup in the storage formation at the end of the injection period is less than the sustainable pressure buildup, the designated storage scenario is not pressure-constrained, and we refer to  $E$  as the *actual storage efficiency factor*. In contrast, in cases where the simulated pressure buildup exceeds the sustainable pressure buildup (which may occur before reaching the designated injection volume), the storage scenario is pressure-constrained. In such cases, we refer to  $E$  as the *maximum storage efficiency factor*, which corresponds to the sustainable pressure buildup.

### 3.1. Model setup

A two-dimensional radially symmetric model domain was chosen to represent a deep saline aquifer. The storage formation, located at a depth of approximately 1200 m below the ground surface, is 250 m thick and bounded at the top and bottom by sealing units (caprock and baserock) of 60 m thick each. The outer lateral boundary has a no-flow condition. In the base case, the model domain has a radial extent of 20 km, and the sealing units are assumed to be impervious. Carbon dioxide is injected in a zone of 125 m in thickness and 50 m in radial extent. Injection operates over 30 years at a rate of  $120 \text{ kg s}^{-1}$  (i.e., annual rate of 3.8 million tonnes of  $CO_2$ ). The aquifer is initially fully brine-saturated, assuming a hydrostatic fluid pressure distribution. Isothermal conditions are modeled with a uniform temperature of  $45^\circ\text{C}$ . Table 1 lists the assigned values of hydrogeological properties typical of a homogeneous brine aquifer suitable for  $CO_2$  storage. Note that the brine compressibility is intrinsically taken into account in TOUGH2/ECO2N in terms of density variation with fluid pressure.

**Table 1 – Hydrogeological properties of the storage formation and  $CO_2$  injection rate used in the base-case simulations**

| Properties                                   | Values                |
|--|-----------------------|
| Horizontal permeability ( $\text{m}^2$ )     | $10^{-13}$            |
| Vertical permeability ( $\text{m}^2$ )       | $10^{-13}$            |
| Pore compressibility ( $\text{Pa}^{-1}$ )    | $4.5 \times 10^{-10}$ |
| Porosity                                     | 0.12                  |
| Van Genuchten (1980) $m$                     | 0.46                  |
| van Genuchten $\alpha$ ( $\text{Pa}^{-1}$ )  | $5.1 \times 10^{-5}$  |
| Residual $CO_2$ saturation                   | 0.05                  |
| Residual water saturation                    | 0.30                  |
| $CO_2$ injection rate ( $\text{kg s}^{-1}$ ) | 120                   |

**Table 2 – Numerical simulation runs for different radial extents of storage formation, and different values of permeability and pore compressibility of the storage formation, as well as permeability of the seals**

|                           | Case number | Radial extent (km) | Formation permeability (m <sup>2</sup> ) | Formation compressibility (Pa <sup>-1</sup> ) | Seal permeability (m <sup>2</sup> ) |
|---------------------------|-------------|--------------------|--|---|-------------------------------------|
| Base case                 | Case 1      | 20                 | $1.0 \times 10^{-13}$                    | $4.5 \times 10^{-10}$                         | 0                                   |
| Storage-formation volume  | Case 2      | 10                 | $1.0 \times 10^{-13}$                    | $4.5 \times 10^{-10}$                         | 0                                   |
|                           | Case 3      | 30                 | $1.0 \times 10^{-13}$                    | $4.5 \times 10^{-10}$                         | 0                                   |
|                           | Case 4      | 50                 | $1.0 \times 10^{-13}$                    | $4.5 \times 10^{-10}$                         | 0                                   |
|                           | Case 5      | 100                | $1.0 \times 10^{-13}$                    | $4.5 \times 10^{-10}$                         | 0                                   |
| Formation permeability    | Case 6      | 20                 | $1.0 \times 10^{-12}$                    | $4.5 \times 10^{-10}$                         | 0                                   |
|                           | Case 7      | 20                 | $5.0 \times 10^{-14}$                    | $4.5 \times 10^{-10}$                         | 0                                   |
| Formation compressibility | Case 8      | 20                 | $1.0 \times 10^{-13}$                    | $4.5 \times 10^{-09}$                         | 0                                   |
|                           | Case 9      | 20                 | $1.0 \times 10^{-13}$                    | $4.5 \times 10^{-11}$                         | 0                                   |
| Seal permeability         | Case 10     | 20                 | $1.0 \times 10^{-13}$                    | $4.5 \times 10^{-10}$                         | $1.0 \times 10^{-20}$               |
|                           | Case 11     | 20                 | $1.0 \times 10^{-13}$                    | $4.5 \times 10^{-10}$                         | $1.0 \times 10^{-19}$               |
|                           | Case 12     | 20                 | $1.0 \times 10^{-13}$                    | $4.5 \times 10^{-10}$                         | $1.0 \times 10^{-18}$               |
|                           | Case 13     | 20                 | $1.0 \times 10^{-13}$                    | $4.5 \times 10^{-10}$                         | $1.0 \times 10^{-17}$               |

The capacity of CO<sub>2</sub> storage in a closed or semi-closed system depends on the hydrogeological properties of the storage formation and the confining units (e.g., permeability, porosity, and pore compressibility), and the total pore volume of the storage formation (e.g., thickness and radial extent). The sensitivity simulations conducted in this study are listed in Table 2. In each sensitivity case, only the property of interest was changed from the base-case value. The van Genuchten model was used to calculate the capillary pressure and the relative permeabilities for the two-phase flow in all the simulation cases (Van Genuchten, 1980). This model contains two fitting parameters  $\alpha$  and  $m$ ; the van Genuchten  $\alpha$  parameter represents the inverse of the characteristic capillary pressure or roughly of the entry pressure for the nonwetting phase and the van Genuchten  $m$  parameter is a measure of the pore-size distribution. The  $\alpha$  and  $m$  values of the storage formation used in the simulations are  $5.1 \times 10^{-5} \text{ Pa}^{-1}$  and 0.46, respectively (Table 1). In Cases 10–13 with imperfect seals, the seal porosity and  $\alpha$  parameter are 0.05 and  $5.1 \times 10^{-6} \text{ Pa}^{-1}$ , respectively. All other properties of the seals are identical to the storage formation. In the model, fixed hydrostatic pressure conditions are set at the top of the upper seal and the bottom of the lower seal.

### 3.2. Results and discussion

Fig. 2a and b show the spatial distributions of CO<sub>2</sub> saturation and pressure buildup (compared to the initial hydrostatic pressure) at the end of the 30-year injection period for the base case. The CO<sub>2</sub> plume is approximately 4 km wide and is concentrated at the top portion of the aquifer, a result of the buoyant CO<sub>2</sub> accumulating below the impervious caprock. As shown in Fig. 2b, the region of elevated pressure is much larger than the CO<sub>2</sub> plume size. In fact, a substantial pressure increase is observed throughout the entire 20 km model domain, with the pressure buildup at the outer radial boundary at approximately 4.5 MPa. The pressure buildup near the injection zone is slightly higher than 6.0 MPa, thus exceeding the assumed sustainable threshold. Notice that the pressure-buildup contour lines away from the CO<sub>2</sub> plume region are mostly vertical, indicating horizontal brine dis-

placement. Nonvertical contour lines can be seen in the CO<sub>2</sub> plume region, where the pressure conditions are affected by buoyancy and nonlinearity inherent in two-phase flow processes. We may conclude that this example features a pressure-constrained formation near or slightly beyond its capacity limits at the end of the designated injection time.

Radial pressure-buildup profiles at different times throughout the injection period are shown in Fig. 3. At the very beginning of injection, the injected CO<sub>2</sub> displaces native brine in the area very close to the injection zone. The strong initial pressure-buildup results from: (1) the driving forces needed to move native brine away from the injection zone and (2) phase interference between aqueous and CO<sub>2</sub> phases in the region of two-phase flow (Pruess and Garcia, 2002). This pressure increase, referred to here as *injection-driven pressure buildup*, depends on the boundary condition (i.e., CO<sub>2</sub> injection rate in the injection zone, injection strategy), formation permeability, and two-phase flow conditions. The pressure pulse propagates away from the injection zone and reaches the outer radial boundary after approximately 2 years. After that, the pressure at the outer boundary starts to increase with injection time in an approximately linear manner; i.e., the entire model domain becomes overpressurized such that additional pore volume is made available to store the injected CO<sub>2</sub>. The pressure buildup related to the need for generating additional pore space is referred to as *storage-driven pressure buildup*, which depends mainly on the pore compressibility of the formation (as well as on changes in brine density).

Cases 1–5 analyze different storage-formation sizes, with radial extent ranging from 10 to 100 km, including scenarios that range from clearly pressure-constrained to not pressure-constrained for the given injection volume. Fig. 2c and d show the spatial distribution of CO<sub>2</sub> saturation and pressure buildup at the end of the 30-year injection period for the case of a domain of 100 km radial extent. Comparison of Fig. 2a and c indicates that the CO<sub>2</sub> plumes in both cases are generally similar in shape, with minor differences in the lateral extent of the plumes caused by differences in pressure buildup and thus CO<sub>2</sub> density. In contrast to the small difference in CO<sub>2</sub> plume extent, a significant difference in the pressure conditions is observed in Fig. 2b and d. The larger model domain is not

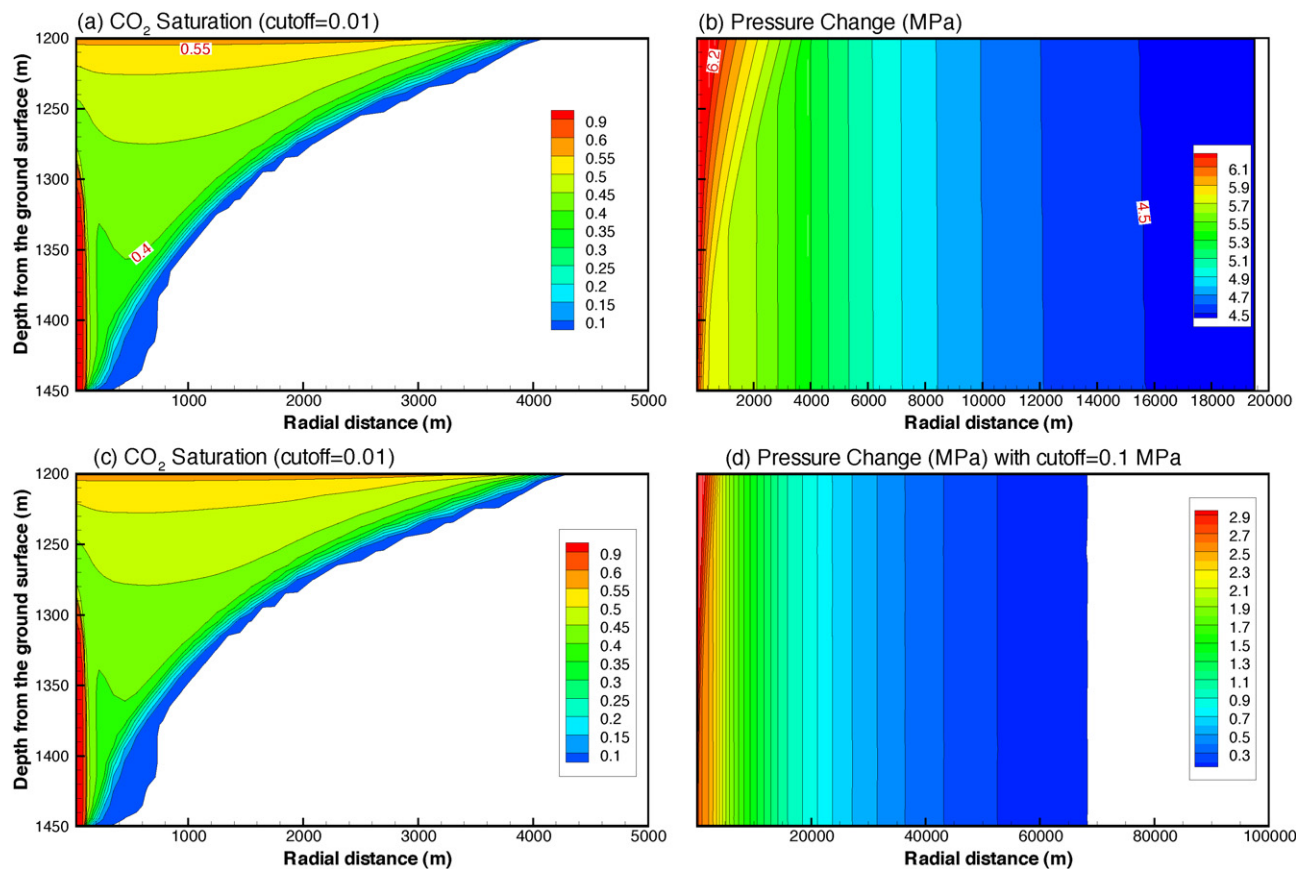


Fig. 2 – Spatial distributions, simulated at 30 years of CO<sub>2</sub> injection, of (a) CO<sub>2</sub> saturation and (b) pressure buildup for the base case with the closed domain of a 20 km radial extent, and (c) CO<sub>2</sub> saturation and (d) pressure buildup for the case of a closed domain of 100 km radial extent. (a) and (c) show close-ups of the CO<sub>2</sub> plume region with two-phase flow of CO<sub>2</sub> and brine.

pressure-constrained, representing the pressure conditions of an open system. As a result, the maximum pressure increase near the injection zone, about half of which is observed in the 20 km case, mainly represents injection-driven pressure buildup. At a radial distance of 20 km, the pressure buildup

is 0.8 MPa in the 100 km case, significantly lower than the 4.5 MPa observed in the 20 km case. In the 10 km case (not shown), the simulated total pressure buildup actually reaches an unrealistically high level at the end of 30-year injection, with maximum values above 18.0 MPa. Injection would have to cease after approximately 8 years to keep the actual pressure buildup smaller than the sustainable threshold of 6.0 MPa.

Fig. 4 shows the sensitivity of local pressure buildup near the injection zone to the permeability and pore compressibility of the storage formation. For the case with higher permeability (one order of magnitude higher than the base case), the pressure buildup in the formation is almost uniform over the entire domain, varying from 5.1 MPa close to the injection zone to 4.7 MPa at the outer boundary (Fig. 4a). For the second case with a lower permeability (a factor of two lower than the base case), a strong local pressure buildup near the injection zone leads to fluid pressure buildup in excess of the assumed sustainable threshold of 6.0 MPa—see Fig. 4b. As a result, the permeability of the storage formation influences both the uniformity of pressure buildup over the domain and the propagation velocity of the pressure pulse away from injection zone. This behavior can be explained easily using the two-dimensional radial flow equation (i.e., the diffusivity equation for pressure propagation), and the diffusivity defined

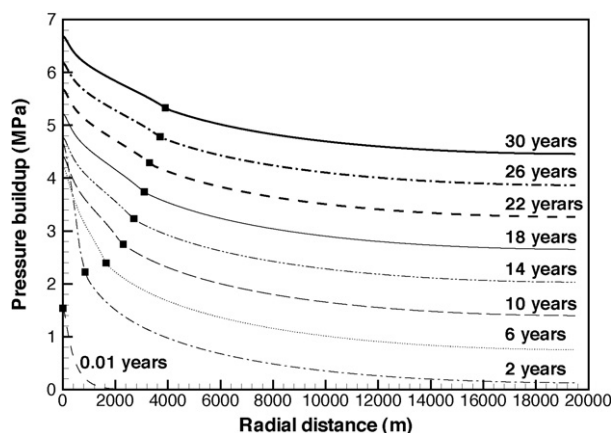
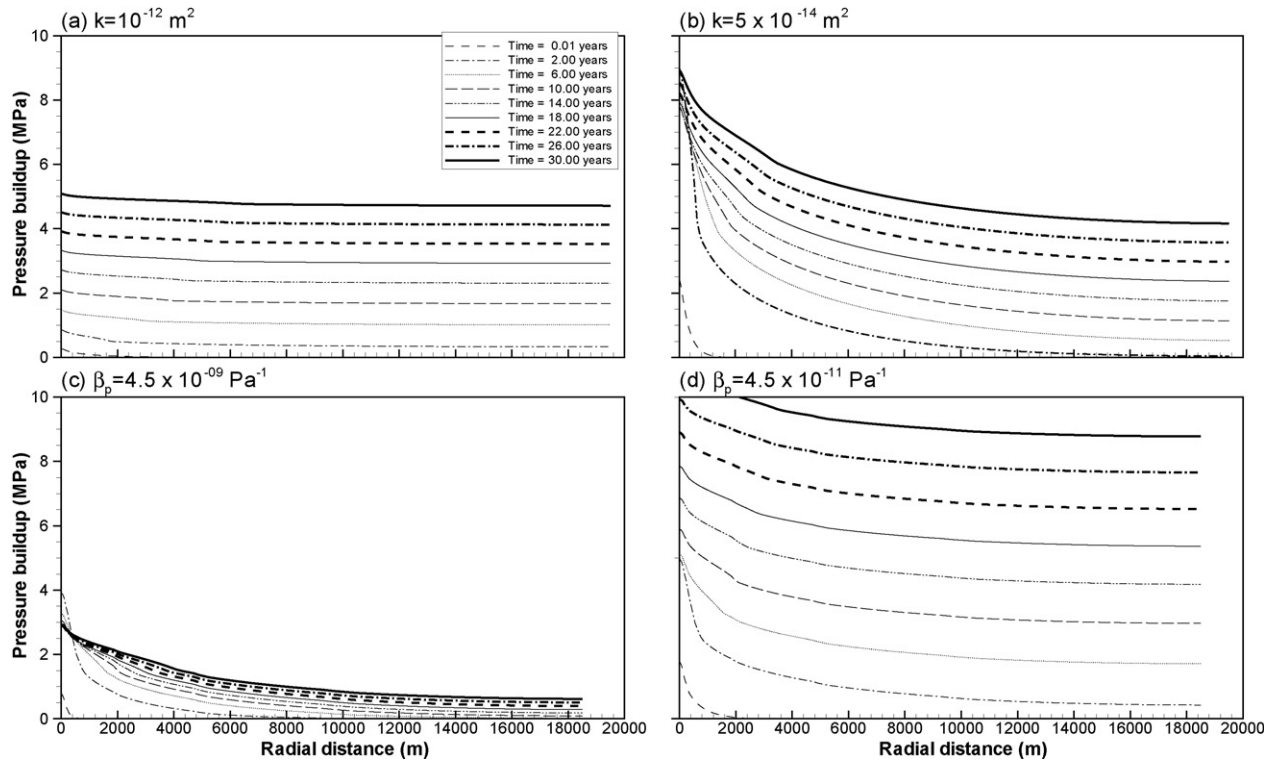


Fig. 3 – Pressure-buildup profiles along the aquifer top at different injection times. Filled squares indicate the CO<sub>2</sub> plume extent to show the radial extent of the evolving two-phase flow region.



**Fig. 4 – Horizontal profiles of pressure buildup at different times of CO<sub>2</sub> injection for formation permeability of (a)  $10^{-12}$  and (b)  $5 \times 10^{-14} \text{ m}^2$ , and pore compressibility of (c)  $4.5 \times 10^{-9}$  and (d)  $4.5 \times 10^{-11} \text{ Pa}^{-1}$ . All other parameters are kept the same as the base case. See comparison with Fig. 3.**

by  $D_d = k/[\phi_t(\beta_w + \beta_p)\mu_w]$ , neglecting the two-phase flow within the CO<sub>2</sub> plume (de Marsily, 1986; Muggeridge et al., 2004). Pressure dissipates (diffuses) faster for higher permeability and/or lower compressibility.

As shown in Fig. 4c and d, the domain-averaged pressure buildup at 30 years is 0.8 and 9.0 MPa for the pore compressibility of  $4.5 \times 10^{-9}$  and  $4.5 \times 10^{-11} \text{ Pa}^{-1}$ , respectively. This indicates that for the case of lower pore compressibility, the system will be pressure-constrained, and the designated CO<sub>2</sub> mass cannot be safely injected into the closed system without geomechanical damage. The pore compressibility of the storage formation is a key input parameter in the quick-assessment method. Wide ranges of pore compressibility have been reported in the literature, depending on the subsurface materials (e.g., Fjaer et al., 1991; Domenico and Schwartz, 1998; Hart, 2000; Harris, 2006).

Fig. 5 shows horizontal profiles of pressure buildup at the top of the storage formation, as a function of seal permeability. The pressure buildup observed in the storage formation is very sensitive to increases in seal permeability. While the lowest seal permeability ( $10^{-20} \text{ m}^2$  or  $10^{-5} \text{ mD}$ ) shows a behavior similar to the closed system for the time scale relevant to estimating CO<sub>2</sub> storage capacity (i.e., the injection time period), we see a strong reduction of overall pressure buildup in all other cases, particularly those with permeabilities of  $10^{-18}$  and  $10^{-17} \text{ m}^2$ . In these cases, a significant fraction (e.g., 0.46 and 0.93) of the displaced brine escapes from the storage formation into the seals, and through the seals into the overlying and underlying formations during the injection

period of 30 years, thereby providing additional storage capacity for the injected CO<sub>2</sub> such that less pressure buildup occurs. We have calculated the cumulative fraction of displaced brine escaping from the storage formation relative to the total volume of stored CO<sub>2</sub> at in situ conditions. With a seal permeability of  $10^{-20} \text{ m}^2$  ( $10^{-5} \text{ mD}$ ), this volume fraction is rather insignificant at 0.07, whereas with a seal permeability of  $10^{-17} \text{ m}^2$  ( $10^{-2} \text{ mD}$ ), this fraction increases to 0.93; i.e., the additional CO<sub>2</sub> storage capacity from brine leakage would amount to about 93% of the total injected CO<sub>2</sub> at 30 years. (In the latter case, the average Darcy's velocity in the seals is approximately  $2.0 \text{ mm year}^{-1}$  for the steady-state condition.) This effect can be very important for storage-capacity estimates in compartmentalized systems that have sealing units with small, but non-zero, permeability. Notice that the pressure profiles in Fig. 5d remain relatively unchanged after a few years of injection, indicating that a quasi-steady state has been reached in which the volumetric rate of leakage of displaced brine is identical to the volumetric rate of injected CO<sub>2</sub> under final storage conditions.

In contrast to the significant leakage of displaced brine, negligible amounts of CO<sub>2</sub> escape from the storage formation into the seals. The cumulative fractions of CO<sub>2</sub> leaking into the caprock are 0.22, 0.35, 0.70, and 3.1% of the total injected CO<sub>2</sub> mass, for the seal permeability cases of  $10^{-20}$  ( $10^{-5} \text{ mD}$ ) to  $10^{-17} \text{ m}^2$  ( $10^{-2} \text{ mD}$ ), respectively. Most of this leakage is dissolved CO<sub>2</sub> that the quick-assessment method cannot account for, migrating with leaking brine from the storage formation into the seals. Carbon dioxide as the nonwetting-



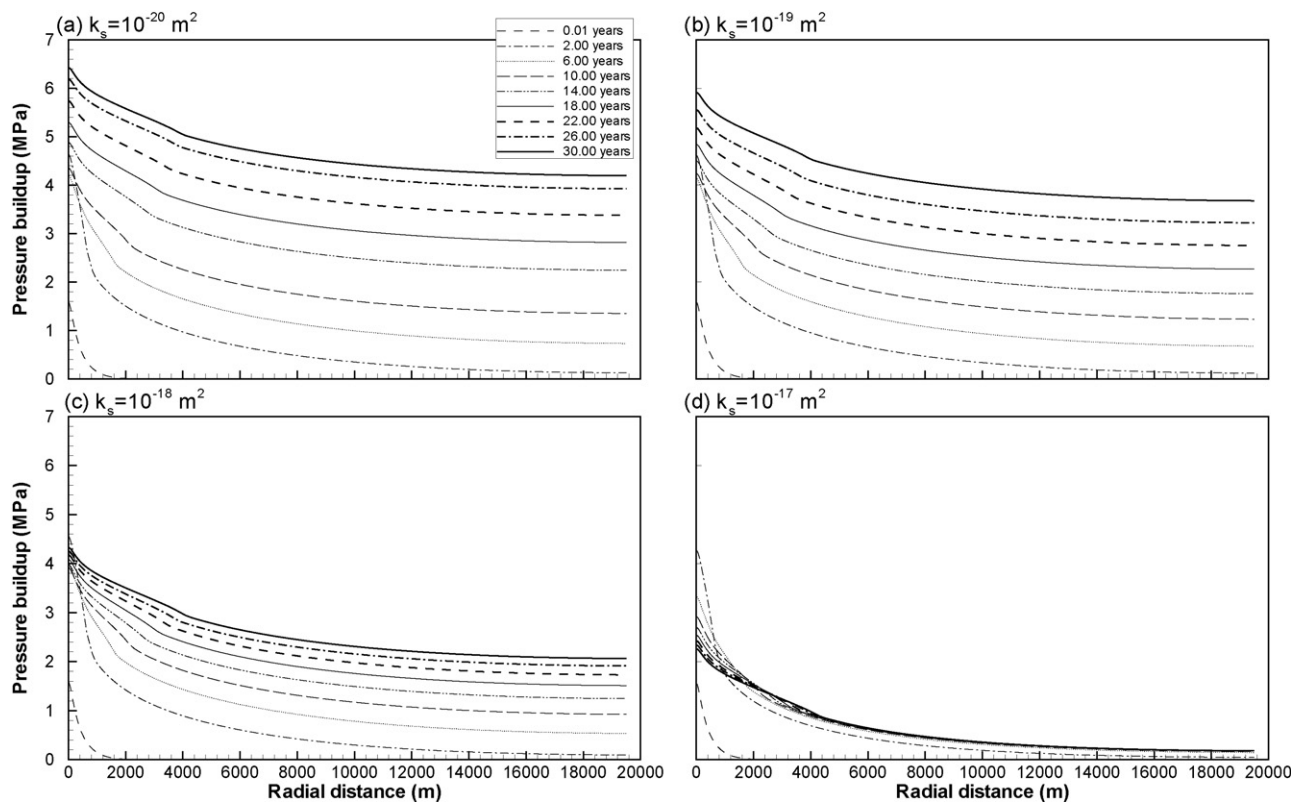


Fig. 5 – Horizontal profiles of pressure buildup along the aquifer top at different times of CO<sub>2</sub> injection for seal permeability of (a)  $10^{-20}$ , (b)  $10^{-19}$ , (c)  $10^{-18}$ , and (d)  $10^{-17}$  m<sup>2</sup>. See comparison with Fig. 3.

phase fluid needs to overcome a considerable capillary entry pressure before being able to migrate into the water-saturated pores of the sealing units. The observed migration of CO<sub>2</sub> within the seals is limited to the immediate vicinity of the storage formation; CO<sub>2</sub> is not able to escape into units overlying or underlying the seals. When a higher entry pressure is used (as represented by a smaller site-specific value of the van Genuchten  $\alpha$  parameter), the CO<sub>2</sub> phase leakage will be smaller.

The simulation results suggest that compartmentalized storage reservoirs with reasonably good, but imperfect, seals may allow for enough displaced brine leaking out of the formation to offset pressure-related storage limitations, while still having sufficient sealing capacity to trap supercritical CO<sub>2</sub>. Seal permeabilities can range over orders of magnitude, from  $10^{-23}$  to  $10^{-16}$  m<sup>2</sup> (Domenico and Schwartz, 1998; Hart et al., 2006; Hovorka et al., 2001; Neuzil, 1994). Relevant to geological CO<sub>2</sub> sequestration, the measured permeability of the sealing unit overlying the storage formation is  $1.0 \times 10^{-18}$  m<sup>2</sup> ( $10^{-3}$  mD) at the Frio test site (Doughty and Pruess, 2004; Hovorka et al., 2001), and 0.75 to  $1.5 \times 10^{-18}$  m<sup>2</sup> at the Sleipner site (Chadwick et al., 2007).

#### 4. Validity of the quick-assessment method

To validate the quick-assessment method, we derived quick estimates of domain-averaged pressure buildup and storage efficiency factors for the simulation scenarios discussed

above, and compared those estimates with their corresponding “true” values obtained via detailed numerical simulations.

##### 4.1. Comparison of pressure-buildup estimates

The first step in demonstrating the validity of the quick-assessment method is to compare the estimated domain-averaged pressure buildup against the numerical simulation results for both closed and semi-closed systems. Fig. 6a shows domain-averaged pressure buildup, as a function of injection time, for closed systems of varying total pore volume (Cases 1–5 in Table 2). The quick-assessment estimates have been obtained using Eq. (4), solving for pressure buildup  $\Delta p(t)$  at given times  $t$  during the injection period. The corresponding cumulative CO<sub>2</sub> volume  $V_{CO_2}(t)$  at each time step  $t$  is derived from the constant CO<sub>2</sub> injection rate of  $120 \text{ kg s}^{-1}$  used in the numerical simulation, and the CO<sub>2</sub> density under the storage condition. Conversion from CO<sub>2</sub> mass to CO<sub>2</sub> volume is conducted at each time step using the CO<sub>2</sub> density calculated at average pressure conditions. The agreement between the true numerical solutions and the quick estimates is excellent, considering that several simplifications and assumptions are involved in the quick-assessment method (e.g., uniform pressure buildup in domain, no dissolution, constant compressibility values). In Case 2, with 10 km radial extent, pressure builds up to values exceeding the sustainable pressure threshold soon after injection.

Fig. 6b and c show domain-averaged pressure buildup for the closed-system cases with varying formation permeability

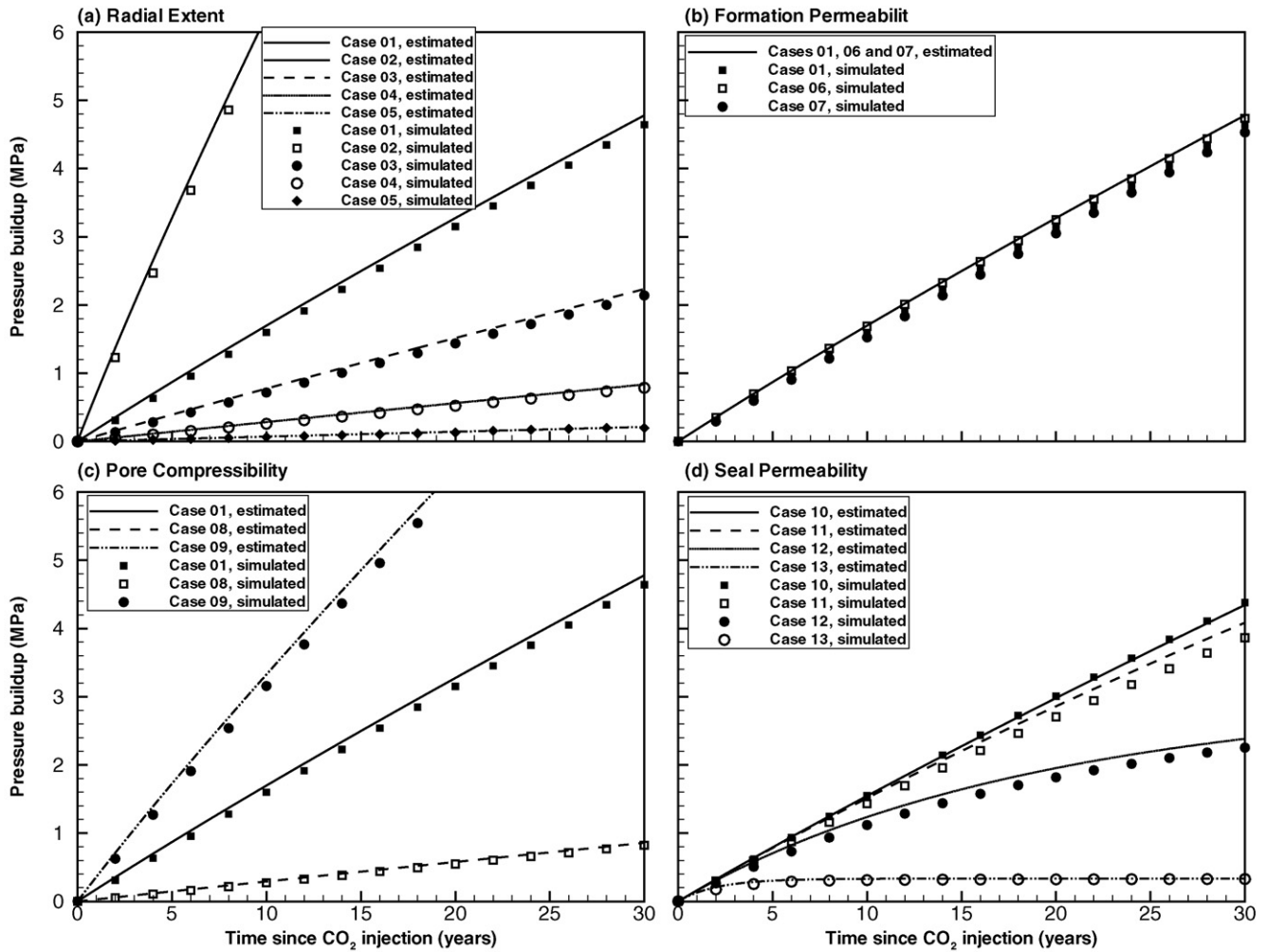


Fig. 6 – Comparison of the transient profiles of domain-averaged pressure buildup obtained through numerical simulations and through the quick-assessment method for (a) a closed system with varying radial extents  $R$ , (b) a closed system with radial extent  $R = 20$  km and varying formation permeability, (c) a closed system with radial extent  $R = 20$  km and varying pore compressibility, and (d) a semi-closed system with radial extent  $R = 20$  km and seals of varying permeability ( $k_s$ ).

(Cases 1, 6, and 7 in Table 2) and varying pore compressibility (Cases 1, 8, and 9 in Table 2), for a radial extent of 20 km. The results of the quick-assessment method are independent of formation permeability, and only one profile obtained by the quick-assessment method is shown in Fig. 6b. The agreement between simulated and estimated average pressure buildup is very good. While formation permeability defines the magnitude of local injection-driven pressure buildup (see Fig. 4), the average pressure change over the entire domain is hardly affected by permeability changes. Pore compressibility, in contrast, has a strong impact on the average pressure buildup in response to  $\text{CO}_2$  injection (Fig. 6c). In the case with the lowest pore compressibility, pressure buildup is so strong that the designated  $\text{CO}_2$  volume cannot be safely stored. Since pore compressibility is a parameter explicitly accounted for in the quick-assessment method, the quick-assessment estimates provide an accurate representation of the detailed simulation results.

Fig. 6d shows a similar comparison of domain-averaged pressure buildup for the semi-closed system with non-ideal

seals of different permeability (Cases 10–13). In these cases, the quick-assessment estimates are obtained using Eq. (6). Overall, the agreement between estimated and numerical results is reasonably good, with a maximum discrepancy of less than 6%. While the quick-assessment method captures well the general transient, nonlinear trends in pressure buildup, it slightly underestimates the pressure buildup for the case with the lowest seal permeability (i.e.,  $10^{-20} \text{ m}^2$  or  $10^{-5} \text{ mD}$ ) and slightly overestimates pressure buildup in the cases with relatively high seal permeability (e.g.,  $10^{-17} \text{ m}^2$  or  $10^{-2} \text{ mD}$ ).

Both numerical and estimated results show clearly that the average pressure approaches an asymptotic maximum after a few years for the case with the relatively high seal permeability of  $10^{-17} \text{ m}^2$  (Fig. 6d). This indicates a steady-state condition with equal volumetric rates of  $\text{CO}_2$  entering and displaced brine leaving the storage formation. We apply Eq. (7) to estimate the average pressure buildup that would correspond to such a condition and arrive at values of 0.34, 3.23, and 27.02 MPa for the three cases with seal permeabilities of  $10^{-17}$ ,  $10^{-18}$ , and  $10^{-19} \text{ m}^2$  ( $10^{-2}$ ,  $10^{-3}$  and  $10^{-4} \text{ mD}$ ), respectively. In the first case, the

estimated value is identical to the final pressure buildup shown in Fig. 6d. In the second case, a steady-state condition has not yet been established after 30 years of injection, but would be reached if injection would continue for a few more years. The pressure value of 3.23 MPa associated with this steady-state condition is less than the sustainable pressure threshold, indicating that this scenario would not be pressure-constrained even if the injection period were much longer. In the third case, however, with a seal permeability of  $10^{-19}$  ( $10^{-4}$  mD) or less, a steady-state condition cannot be reached without geomechanical degradation.

In summary, the quick-assessment method provides reliable pressure estimates that can be compared with the sustainable pressure buildup to judge whether the designated volume of CO<sub>2</sub> can be safely stored in a storage formation, with or without vertical interlayer communication with other formations.

#### 4.2. Comparison of storage efficiency factors for closed systems

We now compare the calculated and estimated (actual) storage efficiency factors of CO<sub>2</sub> storage in a closed system with different total pore volume (i.e., radial extents of 10, 20, 30, 50 and 100 km). The estimated values are obtained using Eq. (5) and the pressure buildup calculated from Eq. (4) for the same injection and storage-formation conditions as in the numerical simulations. We calculate the actual storage efficiency factor corresponding to the considered scenarios of injection and observed pressure buildup, regardless of whether this pressure buildup is higher than the sustainable pressure buildup. Notice that the simulated storage efficiency factors include storage contributions from CO<sub>2</sub> in supercritical phase, as well as CO<sub>2</sub> dissolved in brine.

Table 3 shows the comparison of the actual storage efficiency factors for each case after 30 years of injection, indicating reasonable agreement between estimated and calculated results. The quick-assessment estimates are slightly higher than those obtained through detailed numerical simulations. The significant decrease in the actual storage efficiency factor is observed with the increase in the radial extent, because of the decrease in the pressure buildup. In comparison, the maximum storage efficiency factor, calculated using the sustainable pressure buildup of 6.0 MPa and assigned brine and pore compressibilities would be  $E = 0.0048$ .

The calculated actual storage efficiency factors can be evaluated against the maximum storage efficiency factor to check whether the designated CO<sub>2</sub> volume can be safely stored.

#### 4.3. Comparison of storage contributions for semi-closed systems

In this validation exercise, we compare the three volumetric fractions for a semi-closed system obtained through the quick-assessment method (using Eqs. (3a)–(3c)) against those directly derived from the numerical simulations. Table 4 summarizes the results at the end of the 30-year injection period for the different seal permeability cases. Most of the storage capacity is provided by the storage formation when seal permeability is low (e.g., more than 90% for seal permeability of  $10^{-20}$  m<sup>2</sup> or  $10^{-5}$  mD). In contrast, most of the storage capacity is provided by brine escaping through the seals when seal permeability is comparably high (e.g., more than 90% for seal permeability of  $10^{-17}$  m<sup>2</sup> or  $10^{-2}$  mD). In all cases, the match between the simulated and estimated fractions is reasonably good. The largest relative discrepancies occur with respect to the seal storage of brine, because of the assumed linear pressure variation within the seals in the quick-assessment method.

#### 4.4. Adequacy of important assumptions and simplifications

As shown in the above comparisons, the quick-assessment method provides reasonable estimates for the CO<sub>2</sub> storage capacity and pressure buildup in closed and semi-closed saline formations at various conditions. The accuracy of these estimates depends on the degree to which the process-related assumptions are satisfied in a real problem. One assumption is that the pressure buildup throughout the entire storage formation is uniform. This assumption works well as long as the average pressure is reasonably representative of the true pressure conditions (or, in other words, if the injection-driven pressure buildup is less important than the storage-driven pressure buildup). The detailed simulations in Section 3.2 feature one sensitivity case with small formation permeability of  $5 \times 10^{-14}$  m<sup>2</sup> (50 mD), where injection pressure alone exceeds the sustainable threshold. The quick-assessment method is not applicable in this case.

**Table 3 – Comparison of the actual storage efficiency factors for CO<sub>2</sub> storage in closed systems, obtained through numerical simulation results and the quick-assessment method in Eq. (5), at 30 years of injection**

| Domain radius (km) | Initial pore volume ( $10^9$ m <sup>3</sup> ) | Simulation-based results   |   |                                  | Quick-assessment estimates       |  |
|--------------------|---|--|---|----------------------------------|----------------------------------|--|
|                    |   | Total stored CO <sub>2</sub> volume <sup>a</sup> ( $10^9$ m <sup>3</sup> ) | Average pressure buildup $\Delta p$ (MPa) | Actual storage efficiency factor | Actual storage efficiency factor |  |
| 100                | 942.5   | 0.139  | 0.2                                       | 0.00015                          | 0.00017                          |  |
| 50                 | 235.6   | 0.138  | 0.79                                      | 0.00059                          | 0.00066                          |  |
| 30                 | 84.8  | 0.136  | 2.14                                      | 0.0016                           | 0.0018                           |  |
| 20                 | 37.7  | 0.131  | 4.64                                      | 0.0035                           | 0.0039                           |  |
| 10                 | 9.4   | 0.117  | 16.60 <sup>b</sup>                        | 0.0124                           | 0.014 <sup>b</sup>               |  |

<sup>a</sup> Injected mass is identical for all domains. Stored volumes differ slightly because of different pressure/density conditions.

<sup>b</sup> Average pressure buildup is higher than sustainable threshold. The calculated actual storage efficiency is therefore not feasible.

**Table 4 – Comparison between simulated and estimated volumetric fractions of displaced brine stored in the storage formation, in the seals, and in the overlying and underlying formations, relative to the total pore volume occupied by CO<sub>2</sub> at the end of the 30-year injection period, for different seal permeability values**

| Seals permeability (m <sup>2</sup> ) | Simulation results |       |                  | Estimation by Eqs. (3) |       |                  |
|--------------------------------------|--------------------|-------|------------------|------------------------|-------|------------------|
|                                      | Storage formation  | Seals | Other formations | Storage formation      | Seals | Other formations |
| 10 <sup>−17</sup>                    | 0.071              | 0.011 | 0.918            | 0.069                  | 0.007 | 0.925            |
| 10 <sup>−18</sup>                    | 0.470              | 0.104 | 0.426            | 0.500                  | 0.050 | 0.450            |
| 10 <sup>−19</sup>                    | 0.824              | 0.150 | 0.026            | 0.850                  | 0.085 | 0.065            |
| 10 <sup>−20</sup>                    | 0.931              | 0.059 | 0.010            | 0.903                  | 0.090 | 0.007            |

We generally recommend judging the quick-assessment results with care, knowing that average pressure predictions may underestimate the local conditions near the injection zone. On the other hand, the assumption of negligible CO<sub>2</sub> dissolution leads to an overestimation of pressure buildup and an underestimation of CO<sub>2</sub> storage capacity. The resultant approximation error depends on the CO<sub>2</sub> solubility in brine (which in turn varies with pressure, temperature, and salinity) and the fraction of CO<sub>2</sub> in contact with water. The detailed numerical simulations presented in this study suggest that the mass fraction of CO<sub>2</sub> dissolved in brine ranges from 0.02 to 0.03, and that the dissolved CO<sub>2</sub> accounts for approximately 7% of the total injected CO<sub>2</sub> mass at the end of 30-year injection.

Carbon dioxide density is calculated based on the estimated domain-averaged pressure buildup at storage conditions and the initial hydrostatic pressure. The density calculation captures transient pressure changes, but still introduces some inaccuracies because the domain-averaged pressure buildup may differ from actual pressure conditions within the CO<sub>2</sub> plume (which, of course, define CO<sub>2</sub> density). For native brine, the assumption of constant viscosity and compressibility leads to negligible errors over the pressure range relevant in this study.

## 5. Summary and conclusions

We evaluated the CO<sub>2</sub> storage capacity in compartmentalized structures, where potential storage formations are bounded laterally and by overlying/underlying seals. If CO<sub>2</sub> is injected at an industrial scale into such closed systems (with impervious seals) or semi-closed systems (with non-ideal seals), pressure buildup can have a limiting effect on CO<sub>2</sub> storage capacity. We developed a simple quick-assessment method to assess the expected pressure buildup and CO<sub>2</sub> storage capacity in such potentially pressure-constrained systems. For validation of the method, we used “true” results from a numerical simulation model, which captures all relevant multiphase processes, determining the transient pressure buildup and CO<sub>2</sub> plume evolution in a hypothetical two-dimensional radial system.

The validity of the proposed method was demonstrated by the good agreement between the simple estimates and the numerical results regarding: (1) the pressure-buildup history over the injection period and (2) the storage efficiency factor calculated at the end of the injection period. We consider the new method useful for site selection and characterization, when storage capacity estimates may have to be compared over a large number of sites. For a storage formation of

relatively low permeability, the quick-assessment method may not be suitable because of low injectivity and high degree of non-uniformity of the pressure field, and detailed numerical simulations are required.

One interesting finding of this research is the importance of upper- and lower-seal permeability on pressure buildup in the storage formation. Closed systems with impermeable seals allow CO<sub>2</sub> storage only up to the point at which pressure in the storage formation approaches a sustainable threshold. This pressure constraint translates into small storage efficiency, on the order of 0.5% of the initial pore space for a typical pore compressibility value. However, only storage-formation-seal systems with very low seal permeabilities of 10<sup>−20</sup> m<sup>2</sup> or less exhibit such a closed-system behavior at the time scale of interest to capacity estimation; i.e., the leakage of native brine into and through the bounding seals is so small that the observed pressure buildup is similar to a closed system. With seal permeability varying from 10<sup>−19</sup> to 10<sup>−17</sup> m<sup>2</sup>, brine leakage into and through the seals had a moderate to strong effect in reducing or limiting the pressure buildup in the storage formation, thus allowing for considerably higher storage efficiency, while CO<sub>2</sub> was still safely trapped because of the combined capillary and permeability barriers. Our results indicate that a semi-closed system with seal permeability of 10<sup>−17</sup> m<sup>2</sup> is essentially an open system with respect to pressure buildup, because the rate of displaced brine leaking through the seals equals the rate of injected CO<sub>2</sub> at a later time of injection.

## Acknowledgments

The authors wish to thank Curtis M. Oldenburg at Lawrence Berkeley National Laboratory (LBNL) for his careful internal review of the manuscript. Thanks are also due to Dr. Stefan Bachu, the Associate Editor, and two anonymous reviewers for their constructive suggestions for improving the quality of the manuscript. This work was funded by the Assistant Secretary for Fossil Energy, Office of Sequestration, Hydrogen, and Clean Coal Fuels, National Energy Technology Laboratory, of the U.S. Department of Energy, and by Lawrence Berkeley National Laboratory under Contract No. DE-AC02-05CH11231.

## REFERENCES

- Allis, R., Chidsey, T., Gwynn, W., Morgan, C., White, S., Adams, M., Moore, J., 2001. Natural CO<sub>2</sub> reservoirs on the Colorado



- Plateau and Southern Rocky Mountains: candidates for CO<sub>2</sub> sequestration. In: Proceedings of the First National Conference of Carbon Sequestration, National Energy Technology Laboratory, Washington, DC, USA, May 15–17, 2001.
- Bachu, S., 2002. Sequestration of CO<sub>2</sub> in geological media in response to climate change: road map for site selection using the transform of the geological space into the CO<sub>2</sub> phase space. *Energy Convers. Manage.* 43, 87–102.
- Bachu, S., Adams, J.J., 2003. Sequestration of CO<sub>2</sub> in geological media in response to climate change: capacity of deep saline aquifers to sequester CO<sub>2</sub> in solution. *Energy Convers. Manage.* 44, 3151–3175.
- Bachu, S., Gunter, W.D., Perkins, E.H., 1994. Aquifer disposal of CO<sub>2</sub>: hydrodynamic and mineral trapping. *Energy Convers. Manage.* 35 (4), 269–279.
- Birkholzer, J.T., Zhou, Q., Rutqvist, J., Jordan, P., Zhang, K., Tsang, C.-F., 2007. Research project on CO<sub>2</sub> geological storage and groundwater resources: large-scale hydrogeological evaluation and impact on groundwater systems. Report LBNL-63544, Lawrence Berkeley National Laboratory, Berkeley, CA, USA.
- Bradshaw, J., Bachu, S., Bonijoly, D., Burruss, R., Holloway, S., Christensen, N.P., Mathiassen, O.M., 2007. CO<sub>2</sub> storage capacity estimation: issues and development of standards. *Int. J. Greenhouse Gas Control* 1 (1), 62–68.
- Chadwick, A., Arts, R., Bernstone, C., May, F., Thibeau, S., Zweigel, P., 2007. Best practice for the storage of CO<sub>2</sub> in saline aquifers: observations and guidelines from the SACS and CO2STORE Projects.
- de Marsily, G., 1986. *Quantitative Hydrogeology*. Academic Press, Inc., San Diego.
- Domenico, P.A., Schwartz, F.W., 1998. *Physical and Chemical Hydrogeology*, 2nd ed. John Wiley & Sons, Inc, New York.
- Doughty, C., Pruess, K., 2004. Modeling supercritical carbon dioxide injection in heterogeneous porous media. *Vadose Zone J.* 3, 837–847.
- Fjaer, E., Holt, R.M., Horsrud, P., Raaen, A.M., 1991. *Petroleum Related Rock Mechanics*. Elsevier, Amsterdam.
- Harris, J.M., 2006. Seismic monitoring of CO<sub>2</sub> sequestration. GCEP Technical Report. Stanford University, Palo Alto, CA, USA.
- Hart, D.J., 2000. Laboratory measurements of poroelastic constants and flow parameters and some associated phenomena. Ph.D. Thesis. University of Wisconsin-Madison, Madison, WI, USA.
- Hart, D.J., Bradbury, K.R., Feinstein, D.T., 2006. The vertical hydraulic conductivity of an aquitard at two spatial scales. *Ground Water* 44 (2), 201–211.
- Holloway, S., Heederik, J.P., van der Meer, L.G.H., Czemichowski-Lauriol, I., Harrison, R., Lindeberg, E., Summerfield, I.R., Rochelle, C., Schwarzkopf, T., Kaarstad, O., Berger, B., 1996. The underground disposal of carbon dioxide: summary report. JOULE II Project No. CT92-0031. British Geological Survey, Keyworth, UK.
- Hovorka, S.D., Doughty, C., Knox, P.R., Green, C.T., Pruess, K., Benson, S.M., 2001. Evaluation of brine-bearing sands of the Frio formation, upper Texas gulf coast for geological sequestration of CO<sub>2</sub>. In: First National Conference on Carbon Sequestration, National Energy Technology Laboratory, Pittsburgh, PA, USA, May 14–17, 2001.
- IPCC (Intergovernmental Panel on Climate Change), 2005. *IPCC Special Report on Carbon Dioxide Capture and Storage*. Cambridge University Press, New York.
- Koide, H., Tazaki, Y., Noguchi, Y., Nakayama, S., Iijima, M., Ito, K., Shindo, Y., 1992. Subterranean containment and long-term storage of carbon dioxide in unused aquifers and in depleted natural gas reservoirs. *Energy Convers. Manage.* 33 (5–8), 619–626.
- Muggeridge, A., Abacioglu, Y., England, W., Smalley, C., 2004. Dissipation of anomalous pressures in the subsurface. *J. Geophys. Res.* 109, B11104, doi:10.1029/2003JB002922.
- Neuzil, C.E., 1994. How permeable are clays and shales? *Water Resour. Res.* 30 (2), 145–150.
- Neuzil, C.E., 1995. Abnormal pressures as hydrodynamic phenomena. *Am. J. Sci.* 295, 742–786.
- Neuzil, C.E., 2003. Hydromechanical coupling in geologic processes. *Hydrogeol. J.* 11, 41–83, doi:10.1007/s10040-002-0230-8.
- Nicot, J.-P., 2008. Evaluation of large-scale CO<sub>2</sub> storage on fresh-water sections of aquifers: an example from the Texas Gulf Coast Basin. *Int. J. Greenhouse Gas Control* (in revision).
- Pearce, J.M., Holloway, S., Wacker, H., Nelis, M.K., Rochelle, C., Bateman, K., 1996. Natural occurrence as analogues for the geological disposal of carbon dioxide. *Energy Convers. Manage.* 37 (6–8), 1123–1128.
- Polak, S., Lundin, E., Bøe, R., Lindeberg, E.G.B., Olesen, O., Zweigel, P., 2004. Storage potential for CO<sub>2</sub> in the Beitstadfjord Basin, Mid-Norway. Report SINTEF No. 54.5272.00/01/04 and NGU No. 2004.036. 51 p. Geological Survey of Norway, Trondheim, Norway.
- Pruess, K., 2005. ECO2N: A TOUGH2 fluid property module for mixtures of water, NaCl, and CO<sub>2</sub>. Report LBNL-57952, Lawrence Berkeley National Laboratory, Berkeley, CA, USA.
- Pruess, K., Garcia, J., 2002. Multiphase flow dynamics during CO<sub>2</sub> disposal into saline aquifers. *Environ. Geol.* 42, 282–295.
- Pruess, K., Oldenburg, C.M., Moridis, G., 1999. TOUGH2 user's guide, version 2.0. Report LBNL-43134, Lawrence Berkeley National Laboratory, Berkeley, CA, USA.
- Pruess, K., Garcia, J., Kovscek, T., Oldenburg, C.M., Rutqvist, J., Steefel, C., Xu, T., 2004. Code intercomparison builds confidence in numerical simulation models for geologic disposal of CO<sub>2</sub>. *Energy* 29 (9/10), 1431–1444.
- Puckette, J., Al-Shaieb, Z., 2003. Naturally underpressured reservoirs: applying the compartment concept to the safe disposal of liquid waste. In: Search and Discovery Article 40071, Online Adaptation of Presentation at American Association of Petroleum Geologists, Southwest Section Meeting, Fort Worth, TX, USA, March, 2003 ([www.southwestsection.org](http://www.southwestsection.org)).
- Rutqvist, J., Tsang, C.F., 2002. A study of caprock hydromechanical changes associated with CO<sub>2</sub>-injection into a brine formation. *Environ. Geol.* 42, 296–305.
- Rutqvist, J., Birkholzer, J.T., Cappa, F., Tsang, C.F., 2007. Estimating maximum sustainable injection pressure during geological sequestration of CO<sub>2</sub> using coupled fluid flow and geomechanical fault-slip analysis. *Energy Convers. Manage.* 48, 1798–1807.
- Shafeen, A., Croiset, E., Douglas, P.L., Chatzis, I., 2004. CO<sub>2</sub> sequestration in Ontario, Canada. Part I. Storage evaluation of potential reservoirs. *Energy Convers. Manage.* 45, 2645–2659.
- Stevens, S.H., Pearce, J.M., Rigg, A.A.J., 2001. Natural analog for geologic storage of CO<sub>2</sub>: an integrated global research program. In: Proceedings of the First National Conference of Carbon Sequestration, National Energy Technology Laboratory, Washington, DC, USA, May 15–17, 2001.
- USDOE (U.S. Department of Energy), 2007. Methodology for development of carbon sequestration capacity estimates. Appendix A in Carbon Sequestration Atlas of the United States and Canada. National Energy Technology Laboratory, Pittsburgh, PA, USA.
- USEPA (U.S. Environmental Protection Agency), 1994. Determination of Maximum Injection Pressure for Class I Wells, United States Environmental Protection Agency

- Region 5—Underground Injection Control Section Regional Guidance #7. EPA, Washington, DC, USA.
- Van der Meer, L.G.H., 1992. Investigations regarding the storage of carbon dioxide in aquifers in the Netherlands. *Energy Convers. Manage.* 33 (5–8), 611–618.
- Van der Meer, L.G.H., 1995. The CO<sub>2</sub> storage efficiency of aquifers. *Energy Convers. Manage.* 36 (6–9), 513–518.
- Van Genuchten, M.T., 1980. A closed form equation for predicting the hydraulic conductivity of unsaturated soils. *Soil Sci. Soc. Am. J.* 44, 892–898.